

RESEARCH ARTICLE

Electrical interactions between photoreceptors in the compound eye of *Periplaneta americana*

Paulus Saari^{1,*}, Esa-Ville Immonen^{1,*}, Andrew S. French², Päivi H. Torkkeli², Hongxia Liu², Kyösti Heimonen¹ and Roman V. Frolov^{1,‡}

ABSTRACT

The compound eye of *Periplaneta americana* contains two spectral classes of photoreceptors: narrow-band UV-sensitive and broad-band green-sensitive. In intracellular recordings, stimulation of green-sensitive photoreceptors with flashes of relatively bright UV/violet light produced anomalous delayed depolarization after the end of the normal light response, whereas stimulation of UV-sensitive photoreceptors with green light elicited biphasic responses characterized by initial transient hyperpolarization followed by prolonged delayed depolarization. To explore the basis for these findings, we used RNA interference to selectively suppress expression of the genes encoding green opsin (GO1), UV opsin (UVO) or both. The hyperpolarizing component in UV-sensitive photoreceptors was eliminated and the delayed depolarization was reduced after GO1 knockdown, suggesting that the hyperpolarization represents fast inhibitory interactions between green- and UV-sensitive photoreceptors. Green-sensitive photoreceptor responses of GO1 knockdowns to flashes of UV/violet were almost exclusively biphasic, whereas residual responses to green had normal kinetics. Knockdown of UVO reduced the responses of UV-sensitive photoreceptors but had minor effects on delayed depolarization in green-sensitive photoreceptors. Angular sensitivity analysis indicated that delayed depolarization of green-sensitive photoreceptors by violet light originates from excitation of (an)other photoreceptor(s) in the same ommatidium. The angle at which the maximal delayed depolarization was observed in green-sensitive photoreceptors stimulated with violet light did not match the angle of the maximal transient depolarization. In contrast, no significant mismatch was observed for delayed depolarization elicited by green light. These results suggest that the cellular sources of the normal transient and additional delayed depolarization by violet light are separate and distinct.

KEY WORDS: Cockroach, RNA interference, Ephaptic interactions, Spectral sensitivity, Opsin

INTRODUCTION

In nervous systems, electrical communications between neurons occur via three mechanisms: electrical synapses, chemical synapses and electric field interactions. Direct electrical connections are

mediated by gap junctions and allow propagation of voltage signals rapidly with minimal attenuation. Although extensively regulated, electrical synapses appear to be unsuitable for comprehensive neuronal computation and are only used for ultra-rapid and reliable signal transmission. Chemical synapses represent the main mode of neuronal communication.

Among electric field interactions, two types of effects can be distinguished: relatively high voltage ‘field effects’ caused by synchronous activity of large neuronal populations, and weak local ephaptic interactions caused by electric fields evoked in the extracellular solution during generation and propagation of voltage signals (Kamermans and Fahrenfort, 2004). Opening of ion channels can disturb the ionic concentrations in the surrounding space and create local electrical fields, which may affect membrane potential in the neighboring neurons. Ephaptic interactions remain the least studied mechanism of neuronal communication because they are strongly dependent on the specific neuronal morphology. In both vertebrate and invertebrate visual systems, ephaptic interactions between photoreceptors and between photoreceptors and higher-order neurons are involved in the modulation of signal transmission (Matić, 1983; Shaw, 1975; Vroman et al., 2013).

In this work, we investigated electrical interactions between photoreceptors of the compound eye of *Periplaneta americana*. Cockroach ommatidia contain two spectral classes of photoreceptors, narrow-band UV-sensitive and broad-band green-sensitive (Mote and Goldsmith, 1970, 1971). Recently, three opsin mRNA sequences were discovered in the *Periplaneta* retinal transcriptome (French et al., 2015). One is a typical UV-sensitive r-opsin (UVO) and two are closely related green-sensitive opsins, GO1 and GO2, with GO1 RNA much more abundant than GO2. The GO1 sequence is homologous with the cricket *Gryllus bimaculatus* green opsin type B, which is found throughout the cricket eye, excluding the specialized dorsal rim area (Henze et al., 2012). Expression of opsin genes can be strongly reduced by RNA interference (RNAi), induced by injecting long (>500 bp) double-stranded RNA (dsRNA) into head hemolymph (French et al., 2015).

We found anomalous biphasic responses of UV-sensitive photoreceptors to flashes of green light that were characterized by an initial hyperpolarizing phase followed by strong and prolonged delayed depolarization. We also found delayed depolarization after normal transient responses of green-sensitive photoreceptors to flashes of UV or violet light. To further investigate the basis of these responses, we suppressed expression of genes that code green opsin (GO1) and UV opsin (UVO). Our results suggest that the hyperpolarizing responses are produced by activation of photoreceptors of opposing spectral types within the same ommatidium. However, the origin of delayed depolarization remains unclear. We hypothesize that it might be caused by changes in extracellular ionic concentrations

¹Biophysics group, Nano and Molecular Systems Research Unit, University of Oulu, Oulu 90014, Finland. ²Department of Physiology and Biophysics, Dalhousie University, Halifax, NS, Canada, B3H 4R2.

*These authors contributed equally to this work

‡Author for correspondence (rvfrolov@gmail.com)

© R.V.F., 0000-0002-7431-5297

List of symbols and abbreviations

dsRNA	double-stranded RNA
GO1	green opsin 1
<i>I</i>	light intensity
<i>I</i> ₀	maximal light intensity
LED	light-emitting diode
LJP	liquid junction potential
RNAi	RNA interference
UVO	UV opsin
<i>V</i> _{max}	maximum voltage
$\Delta\phi$	acceptance angle

in the restricted intra-ommatidial space of the fused rhabdom during activation of adjacent photoreceptors.

MATERIALS AND METHODS

American cockroaches [*Periplaneta americana* (Linnaeus 1758)] were purchased from Blades Biological (Blades Biological Ltd, Edenbridge, Kent, UK) and maintained in reversed 12 h:12 h illumination conditions with a subjective 'night' period matching the actual day. Only male cockroaches were used for experiments. Experiments were performed at room temperature (20–22°C).

RNA interference

RNAi was performed using long dsRNA for UVO and GO1 as described previously (French et al., 2015). In brief, reverse transcription was performed using total RNA extracted from cockroach retinas and oligo d(T)23VN primers with ProtoScript II reverse transcription (New England Biolabs). The reverse transcription product was used in PCRs to amplify the template DNAs using Q5 High-Fidelity DNA Polymerase (New England Biolabs). dsRNA was synthesized with the MEGAscript RNAi kit (Ambion, Thermo Fisher Scientific). For application, 4–6 µg of dsRNA in 1 µl of injection buffer (0.1 µmol l⁻¹ Na-phosphate buffer+5 µmol l⁻¹ KCl) was injected with a sterile glass capillary patch electrode through a small hole into the frontal part of the head under CO₂ anesthesia. The microelectrode tip was broken sufficiently to allow easy discharge of its contents when gentle positive pressure was applied through silicone tubing. After the injection, animals were maintained in separate cages at 25°C. Control animals either received no injections or were injected with 1 µl Ringer solution.

Quantification of mRNA expression by real-time quantitative PCR

Effects of UVO knockdown on GO1 and UVO mRNA concentrations were measured by real-time quantitative PCR as described previously (French et al., 2015). In brief, total RNA was extracted from 14–16 retinas of dsRNA, saline-injected and untreated animals 21 days after injection using an RNeasy Plus mini kit (Qiagen). mRNA was evaluated using an Expiration RNA Analysis Kit (Bio-Rad) after treatment with RNase-free DNase I (Ambion). A total of 50 ng of total RNA was used for first-strand cDNA synthesis with ProtoScript II reverse transcriptase (New England BioLabs). Quantitative PCR was performed using GoTaq qPCR Master (Promega) on a CFX96TM real-time PCR detection system (Bio-Rad) as described previously (Immonen et al., 2017). Gene expression levels, PCR efficiency and the standard error of measurement were calculated using CFX Manager (Bio-Rad). Amplification efficiencies of the primers were determined using

serially diluted cDNA samples. All PCR runs were performed in triplicate and the data were analyzed using CFX Manager (Bio-Rad). Opsin and primer sequences for the specific and reference genes are provided elsewhere (French et al., 2015).

Patch-clamp recordings

Recordings were performed from photoreceptors of control or dsRNA-treated cockroaches during days 10 to 20 after injection. Ommatidia were dissociated and whole-cell recordings were performed as described previously (Immonen et al., 2017). In brief, data were acquired using an Axopatch1-D patch-clamp amplifier, a Digidata1550 digitizer and pClamp10 software (Axon Instruments/Molecular Devices). Patch electrodes were made from thin-walled borosilicate glass (World Precision Instruments). Electrode resistances were between 5 and 9 MΩ. Bath solution contained (in mmol l⁻¹): 120 NaCl, 5 KCl, 4 MgCl₂, 1.5 CaCl₂, 10 N-Tris-(hydroxymethyl)-methyl-2-amino-ethanesulfonic acid (TES), 25 proline and 5 alanine, pH 7.15. Patch pipette solution contained (in mmol l⁻¹): 100 K-gluconate, 40 KCl, 10 TES, 2 MgCl₂, 4 Mg-ATP, 0.4 Na-GTP and 1 NAD, pH 7.15. The liquid junction potential (LJP) was –12 mV. All voltage values cited in the text were corrected for the LJP. The series resistance was compensated by 80% and did not exceed 10 MΩ. Membrane capacitance was calculated from the total charge flowing during capacitive transients for voltage steps from –112 to –92/–82 mV.

Intracellular recordings

In vivo intracellular single-electrode recordings were performed as described previously (Saari et al., 2017). In brief, the dorsal part of the left compound eye was used in the experiments. Photoreceptor responses were recorded using sharp microelectrodes (borosilicate glass; Harvard Apparatus) manufactured with a laser puller (P-2000; Sutter Instrument) and filled with 2 mol l⁻¹ KCl solution, pH 6.84, to a final resistance of 100–150 MΩ. The reference electrode was placed through the left antenna. Signals were recorded with an intracellular amplifier (SEC-05L; NPI Electronic). All cells used for analysis had resting potentials of –45 mV or lower, with control photoreceptors demonstrating transient depolarization at the zero attenuation of at least 25 mV in amplitude in response to flash or continuous stimulation.

Light stimulation

Light stimulation was performed as described previously (Saari et al., 2017). In brief, a computer-controlled custom-made voltage-to-current driver for light-emitting diodes (LEDs) was used to drive 10 (in patch-clamp experiments) or 14 (in intracellular experiments) LEDs (Roithner Laser Technik, Austria), with narrow-band emission peaks ranging from 355 to 625 nm (355, 385, 400, 435, 450, 462, 490, 505, 525, 545, 572, 594, 612 and 625 nm), which were used in combination with a series of neutral density filters (Kodak). The LED series was calibrated, using a UV-Vis spectrometer USB4000 (Ocean Optics), to have equal photon output at each wavelength. In patch-clamp experiments, the spectral class of photoreceptors was determined using a simple protocol consisting of 20 ms isoquantal flashes of light from all 10 LEDs at an intermediate light intensity. In intracellular experiments, the stimulation was delivered on-axis, and the angular size of the light source was 2.5 deg. Light intensity is presented either as log(*I*/*I*₀), where *I* is the current light intensity and *I*₀ is the highest intensity, for data obtained with the same LED, or as relative photons s⁻¹ for comparison of data obtained at different wavelengths.

Angular and spectral sensitivity measurements

In angular sensitivity measurements, the optical axis of the photoreceptor was determined initially by changing the polar and azimuthal angles of the light source while recording light responses in a Cardan-arm system. A $V\text{-log}(I/I_0)$ function was then obtained from responses to 20 ms pulses delivered on-axis in $10^{0.5}$ increments over a 10^4 intensity range. After correcting the polar angle values for the azimuthal angle, sensitivity values were found in the following way: by fitting the $V\text{-log}(I/I_0)$ function with the Hill equation, the V_{\max} and Hill coefficient N values were acquired. Sensitivity coefficients C_θ at each corrected polar angle θ were then calculated using the equation:

$$C_\theta = \left(\frac{V_\theta/V_{\max}}{1 - V_\theta/V_{\max}} \right)^{\frac{1}{N}}, \quad (1)$$

where V_θ is the corresponding voltage response amplitude, and then normalized by dividing by the largest C_θ , which was usually found at the optical axis, giving relative sensitivities. The acceptance angle $\Delta\theta$ was defined as the half-width of the Gaussian fit to the dependence of relative sensitivity on the corrected polar angle.

Spectral sensitivities of photoreceptors were calculated similarly. First, we measured a $V\text{-log}(I/I_0)$ function with one LED, usually peaking at 525 nm, by recording responses to 20 ms light pulses delivered on-axis in $10^{0.5}$ increments over a 10^4 intensity range. By fitting the functions separately in each cell with a Hill equation, we obtained the V_{\max} and Hill coefficient N values, which were 44.0 ± 4.9 mV and 0.57 ± 0.07 ($n=20$), respectively. Next, voltage responses to a series of isoquantal 20 ms pulses were recorded for all LEDs at an intermediate light intensity that yielded peak depolarizing responses no higher than 30 mV. Relative sensitivities were calculated using Eqn 1, by obtaining spectral sensitivity coefficients for each wavelength and then normalizing them.

Statistics

The Shapiro–Wilk normality test was first applied to data samples to determine whether they could be analyzed using parametric statistical methods. As all our experimental groups passed the normality test, the data are presented as means \pm s.d., unless specified otherwise, and were compared using a two-tailed t -test. Throughout the text, n indicates sample size.

RESULTS

Responses of normal photoreceptors

To evaluate spectral sensitivity in intracellular recording experiments, we used 20 ms isoquantal flashes of light from 14 LEDs, combined with a range of neutral density filters. We found two spectral classes of photoreceptors, consistent with the original study of spectral sensitivity of photoreceptors in cockroach compound eyes (Mote and Goldsmith, 1970). A minority of photoreceptors (<10%) were only sensitive to UV (Fig. 1A, UV-sensitive). Most photoreceptors were characterized by broad spectral sensitivities with maximal responses observed between 490 and 525 nm (Fig. 1B, green-sensitive).

In UV-sensitive photoreceptors, maximal responses were elicited by LEDs with emission peaks at 355 and 385 nm. In the UV-sensitive photoreceptor shown in Fig. 1A, long-wavelength flashes elicited fast and small hyperpolarizing transients, similar to color-opponent responses reported in butterfly photoreceptors (Matić, 1983).

The spectral sensitivity measurements were performed at an intermediate light level. After the end of responses to flashes of UV light, approximately half of the green-sensitive photoreceptors demonstrated anomalous delayed depolarization of varying amplitude (Fig. 1B). Importantly, these depolarizations were observed after responses to UV light characterized by smaller peak amplitudes than responses to green light, which showed no such depolarizations (pink and cyan traces in Fig. 1B).

Fig. 1C demonstrates dependencies of peak depolarization on peak LED wavelength at the same light level for four UV-sensitive photoreceptors (pink traces) and a mean trace for 19 green-sensitive photoreceptors (green trace). Although green-sensitive photoreceptors showed substantial responses to UV and violet light, analysis of spectral sensitivity functions revealed that their maximal UV/violet sensitivity does not exceed the sensitivity predicted by the beta-band of green opsin, which can have a relative magnitude of up to 0.29 (Stavenga et al., 1993). In our experiments, the peak short wavelength sensitivity of green-sensitive photoreceptors was 0.31 ± 0.17 ($n=19$) of the maximal sensitivity in the green part of the spectrum. Fig. 1C (dark green triangles) also shows that there was no difference in the mean action spectrum obtained from photoreceptors of cockroaches injected by saline when compared with those that were not injected. The maximal UV sensitivity in the majority (ca. 80%) of green-sensitive photoreceptors was 385 nm (Fig. 1D), with the rest of green-sensitive photoreceptors showing secondary peaks at 355 nm.

To further investigate the anomalous responses, we stimulated green- and UV-sensitive photoreceptors with 20 ms flashes of green (525 nm) or violet (400 nm) light over a broad range of light intensities in $10^{0.5}$ increments. In these experiments, we used an LED with maximum emission at 400 nm, because 355 and 385 nm LEDs had relatively low photon outputs, preventing investigation of bright backgrounds. Responses recorded from a typical UV-sensitive photoreceptor are shown in Fig. 1E. Thick dark pink and dark green traces indicate responses elicited at the same neutral density filter attenuation level, although the green stimulus had approximately 1.5 times more photons than the violet stimulus. Biphasic responses appeared in relatively dim light, with both hyperpolarization and delayed depolarization amplitudes increasing with light level (Fig. 1E).

In green-sensitive photoreceptors, delayed depolarization appeared at intermediate light levels after stimulation with both 400 and 525 nm stimuli and increased with light intensity (Fig. 1F). Thick cyan and thick dark pink traces correspond to responses to the highest intensity flashes of green and violet light, respectively. Because green-sensitive photoreceptors are much less sensitive to 400 nm than to 525 nm (Fig. 1F), to properly study delayed depolarization at different wavelengths we had to compare responses with equal amplitudes of depolarization. Although stimulation with green light caused substantial delayed depolarization (thick dark green trace, Fig. 1F), the response to violet eliciting a slightly smaller peak was characterized by much stronger delayed depolarization (thick dark pink trace, Fig. 1F).

Fig. 1G shows the dependencies of delayed depolarization (values obtained at 200 ms after onset of the stimulus, dashed line in Fig. 1F) on peak depolarization in green-sensitive photoreceptors stimulated with 20 ms green and violet pulses of light. In all cells, delayed depolarization was stronger for violet stimuli. These results indicate that despite the relatively low sensitivity of green-sensitive photoreceptors to UV/violet light, it produces additional delayed depolarization.

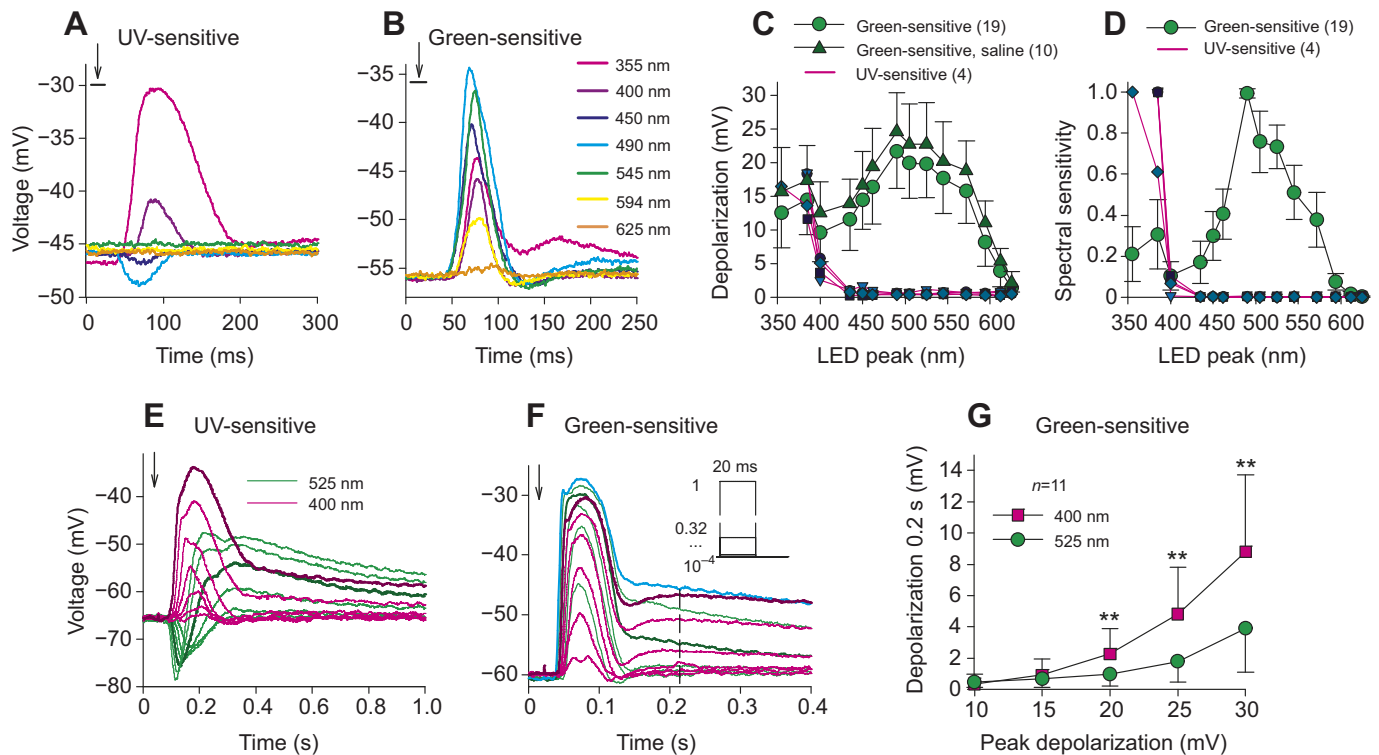


Fig. 1. Normal responses of *Periplaneta americana* photoreceptors in intracellular recordings. Spectral sensitivity was evaluated by applying 20 ms flashes of light from 14 narrow-band LEDs; stimulus intensities were adjusted to emit approximately the same number of photons ('isoquantal' flashes). Here and in all other figures, the stimulus timing is denoted with horizontal bars with or without arrows, or with arrows only for relatively short stimuli. (A) Responses of a UV-sensitive photoreceptor are shown for seven LEDs; color key is in B. (B) Responses of a green-sensitive photoreceptor. (C) Dependencies of voltage transient amplitudes on peak LED wavelength for green-sensitive photoreceptors in control (19 photoreceptors from seven animals) and saline-injected (10 photoreceptors from three animals) cockroaches, and individual responses of four UV-sensitive photoreceptors. Here and in all other figures, numbers in parentheses indicate the number of cells, and error bars represent s.d. (D) Spectral sensitivities of UV- and green-sensitive photoreceptors obtained from action spectra in C. (E) Responses of a UV-sensitive photoreceptor to 20 ms flashes of 525 or 400 nm light over a 10^4 range of light intensities. Dark green and dark pink traces indicate responses to stimuli at the same light level. (F) Responses of a green-sensitive photoreceptor to the same stimuli. Thick dark green and thick dark pink traces are responses with the same peak amplitude; thick cyan and thick dark pink denote responses to the highest intensity flashes of green and violet light, respectively. (G) Inferred dependencies of delayed depolarization on peak depolarization in green-sensitive photoreceptors. Delayed depolarization amplitude was determined at 200 ms after the start of the recording protocol (dashed line in F). As no direct statistical comparison of delayed depolarizations elicited by green and violet stimuli was possible due to data sets incompatibility, we fitted each individual dependence with a Hill equation. Then, using the fitting curves, we obtained fitted delayed depolarization values corresponding to peak depolarizations of 10, 15, 20, 25 and 30 mV; in this analysis, only photoreceptors eliciting responses with maximal transient depolarizations ≥ 30 mV were used. Significant differences indicated with $**P < 0.01$ in paired *t*-test.

To further investigate delayed depolarization, we performed patch-clamp recordings from green-sensitive photoreceptors using 20 ms flashes of UV (355 nm) or green (525 nm) light. In contrast to the results of intracellular experiments (Fig. 1), we found no evidence of any additional depolarization after illumination with bright UV light (Fig. 2).

Effects of *GO1* and *UVO* gene knockdown on green-sensitive photoreceptors

To determine the cause of delayed depolarization in green-sensitive and biphasic responses in UV-sensitive photoreceptors, we knocked down *GO1* and *UVO* genes (*GO1kd* and *UVOkd*, respectively) using RNAi as described previously (French et al., 2015).

Dissociated photoreceptors were investigated using whole-cell patch-clamp recordings in the voltage-clamp mode. Two properties were assessed: absolute sensitivity to light and quantum bump amplitude. Quantum bumps are elementary responses elicited by activation of microvilli by discrete photons. The only change observed in the *GO1kd* photoreceptor properties was a dramatic decrease in absolute sensitivity to green light. Fig. 3A,B shows typical responses of control and *GO1kd* photoreceptors: very

different light intensities were needed to elicit similar bump rates during continuous stimulation. Fig. 3C shows that mean quantum bump amplitude was similar in control and *GO1kd* photoreceptors. These results are similar to previous findings in *Drosophila melanogaster*, where decreased concentration of a specific visual pigment led to reduced absolute sensitivity in terms of bump rate but had no effect on current bump amplitude because the bump current does not depend on the number of visual pigment molecules simultaneously activated by light in each microvilli (Johnson and Pak, 1986).

In intracellular recordings, *GO1kd* green-sensitive photoreceptors had distinct residual responses to short flashes of UV/violet light when compared with the normal photoreceptors (Fig. 4A). They were almost always biphasic, strongly resembling responses of normal UV-sensitive photoreceptors to stimulation with green light (Fig. 1E). In several *GO1kd* and *UVO/GO1kd* photoreceptors, only biphasic responses could be detected. Delayed responses to UV light in these cells had slower onset and longer decay than responses to longer wavelengths (Fig. 4B). Examples of responses of two *GO1kd* photoreceptors to 20 ms flashes of green (525 nm) and violet (400 nm) light over a range of background

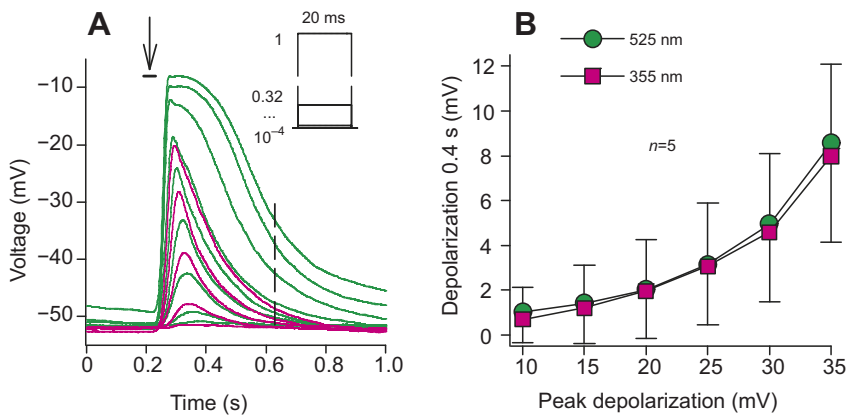


Fig. 2. There was no delayed depolarization in patch-clamp experiments. Dissociated ommatidia were stimulated with 20 ms pulses of either UV (355 nm) or green (525 nm) light in $10^{0.5}$ -fold intensity increments. (A) Typical responses of one photoreceptor. (B) Inferred dependencies of delayed depolarization on peak depolarization for green and UV stimuli; delayed depolarization amplitude was determined at 400 ms after the start of the recording protocol (dashed line in A); values were obtained as in Fig. 1G.

intensities are shown in Fig. 4C,D. Fig. 4C demonstrates a typical result, with fast residual responses to green and strong biphasic responses to violet. Fig. 4D shows unusual results from a photoreceptor characterized by residual fast transients in response to 400 nm stimulus, and delayed depolarization after 525 nm stimulus. Such responses were observed in two out of 16 GO1kd photoreceptors.

To investigate whether the additional delayed depolarization in green-sensitive photoreceptors after stimulation with UV/violet light is caused by interactions between green- and UV-sensitive photoreceptors, we studied responses of green-sensitive photoreceptors after both opsins were suppressed

(GO1/UVOkd). We expected to find decreased amplitudes of delayed depolarization and/or hyperpolarizing transients after stimulation with UV/violet light. Use of double knockdowns was necessary to eliminate or reduce intrinsic responses of green-sensitive photoreceptors to UV/violet light. Fig. 4E shows typical responses of a GO1/UVOkd photoreceptor. Fig. 4F compares mean amplitudes of hyperpolarization and delayed depolarization after stimulation with 20 ms flashes of violet light in GO1kd and GO1/UVOkd photoreceptors. In bright light, the amplitude of delayed depolarization is smaller in GO1/UVOkd than in GO1kd photoreceptors, suggesting that delayed depolarization is indeed partly caused by activation of UV-sensitive photoreceptors.

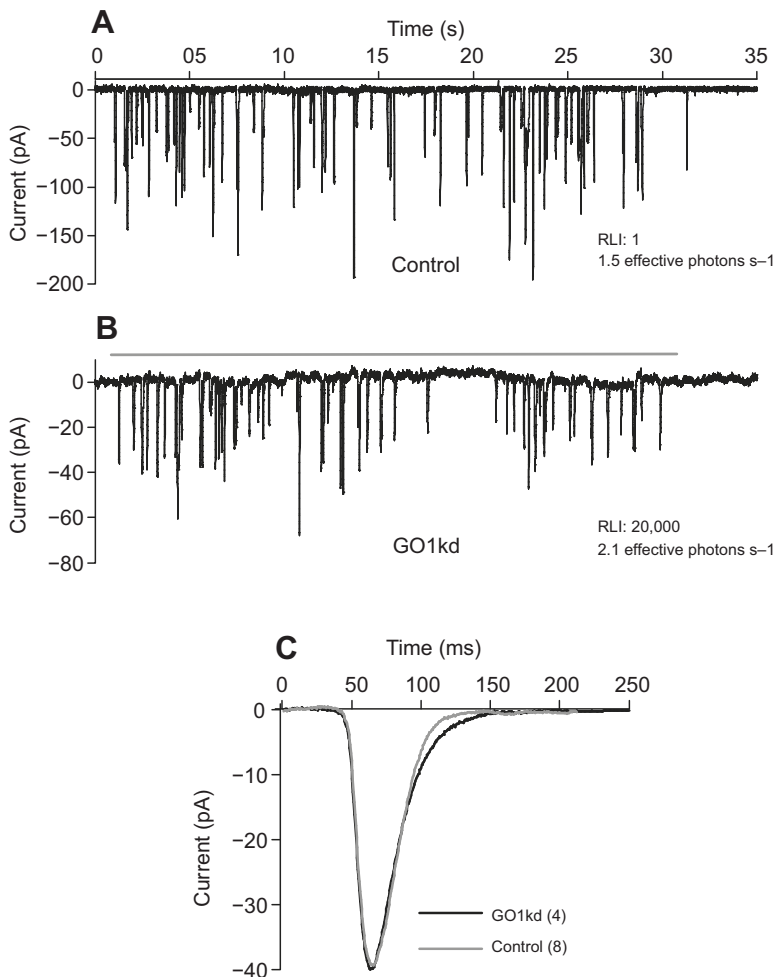


Fig. 3. Knockdown of GO1 decreased absolute sensitivity but not quantum bump amplitudes. Data were obtained from whole-cell patch-clamp experiments. (A,B) Voltage-clamp recordings of current quantum bumps from green-sensitive control (A) and GO1kd (B) photoreceptors from dissociated ommatidia. The stimulus intensity was adequate to evoke 1 to 10 bumps or effective photons s^{-1} . The horizontal gray lines indicate the duration of light stimulus. Recordings from the GO1kd photoreceptors were performed between days 10 and 20 after dsRNA injection; RLI, relative light intensity. (C) Average quantum bumps from control and GO1kd photoreceptors. Average quantum bumps were first found for each photoreceptor and then averaged again.

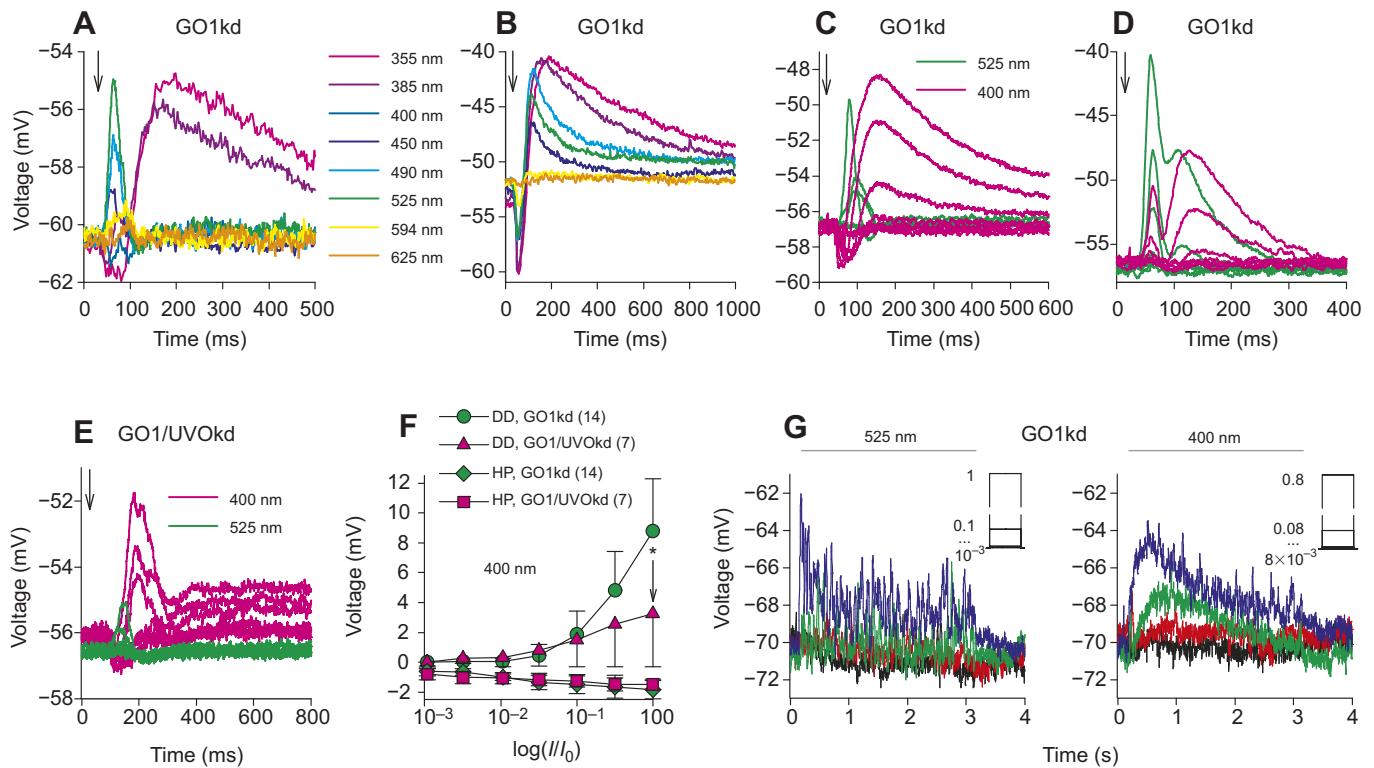


Fig. 4. Effects of knockdown of GO1 and GO1/UVO on green-sensitive photoreceptors. Data were obtained from intracellular experiments. (A) Typical example of responses of a green-sensitive GO1kd photoreceptor to 20 ms isoquantal flashes from 14 LEDs. (B) Responses to the same set of stimuli recorded from another GO1kd photoreceptor characterized by the absence of the typical fast responses. Note that the responses to green light had faster onset and decay kinetics than responses to UV and violet. (C) Responses of a GO1kd photoreceptor to 20 ms flashes of 525 or 400 nm light over a 10^4 range of light intensities. (D) Responses of another GO1kd photoreceptor characterized by the presence of delayed depolarization after stimulation with green light and transient depolarization after stimulation with violet. (E) Responses of a GO1/UVOkd photoreceptor to the same stimuli as in D. (F) In bright light, maximal delayed depolarization after stimulation with 400 nm stimulus was significantly smaller in GO1/UVOkd than in GO1kd photoreceptors (4.3 ± 3.5 , $n=7$ versus 9.1 ± 4.8 mV, $n=14$, $*P=0.022$, unpaired t -test). DD, delayed depolarization; HP, hyperpolarization. (G) Responses of a green-sensitive photoreceptor from a GO1kd to 3 s pulses of either green (left) or violet (right) light; photon flux estimate was ca. 22% higher for each green pulse than for the corresponding violet stimuli.

However, no significant difference was found in the amplitudes of hyperpolarizing transients.

Next, we tested prolonged responses to green and violet stimuli in green-sensitive GO1kd photoreceptors. Fig. 4G shows that responses to 3 s pulses of violet light (right panel) had much slower onsets and different kinetics than responses to green light of similar intensity (left panel).

Because UV-sensitive photoreceptors are very rare in patch-clamp experiments, we investigated UVO knockdowns only in intracellular recordings. Measurement of UVO mRNA concentration by qPCR indicated that knockdown of the *UVO* gene was successful. Fig. 5A demonstrates that after injection of dsRNA targeting *UVO*, its mRNA concentration decreased to 3% of the control value, whereas the mRNA concentration of GO1 did not change significantly. GO1kd was previously shown to reduce concentrations of both GO1 and GO2 mRNA by approximately 99%, but had no effect on UVO mRNA concentration (French et al., 2015).

The transient response amplitudes of green-sensitive UVOkd photoreceptors were similar to that of the control (Fig. 5B,C). Delayed depolarization in green-sensitive UVOkd photoreceptors after stimulation with 20 ms flashes of green or violet light was compared with the control (Fig. 1F). The mean amplitudes of peak depolarization in the two groups matched closely in bright light, but the delayed depolarization was slightly smaller in UVOkd photoreceptors, albeit the differences were not statistically significant (Fig. 5C).

Effects of GO1 and UVO gene knockdowns on UV-sensitive photoreceptors

We hypothesized that biphasic responses originate from electrical activity in the neighboring photoreceptors. As biphasic responses to green light in UV-sensitive photoreceptors were not masked by normal responses, as in green-sensitive photoreceptors stimulated with UV/violet light, we investigated whether the mechanism of biphasic responses could be clarified by knockdown of specific opsins.

In intracellular recordings from UV-sensitive GO1kd photoreceptors, the maximal transient depolarization amplitude of voltage responses to 20 ms flashes of intermediate intensity at 385 nm was 21.5 ± 9.0 mV ($n=13$). In the combined group of UV-sensitive UVOkd ($n=1$) and GO1/UVOkd ($n=4$) photoreceptors, similar flashes depolarized the membrane by 10.2 ± 6.5 mV. This difference was statistically significant (unpaired t -test, $P=0.006$, $n=5$; Fig. 6A). By converting voltage responses into spectral sensitivity values using a mean $V - \log(I/I_0)$ function obtained from UV-sensitive GO1kd photoreceptors, we found that the average maximal UV sensitivity of UV-sensitive photoreceptors in the combined group of UVOkds and GO1/UVOkds decreased by 91%.

In responses to 20 ms isoquantal flashes of light from different LEDs, hyperpolarizing transients were found in UV-sensitive photoreceptors in control (Fig. 1A) and UVOkd (Fig. 6B) but not in GO1/UVOkd (Fig. 6C) or GO1kd cockroaches (Fig. 6D). We also investigated the dependencies of hyperpolarizing transient

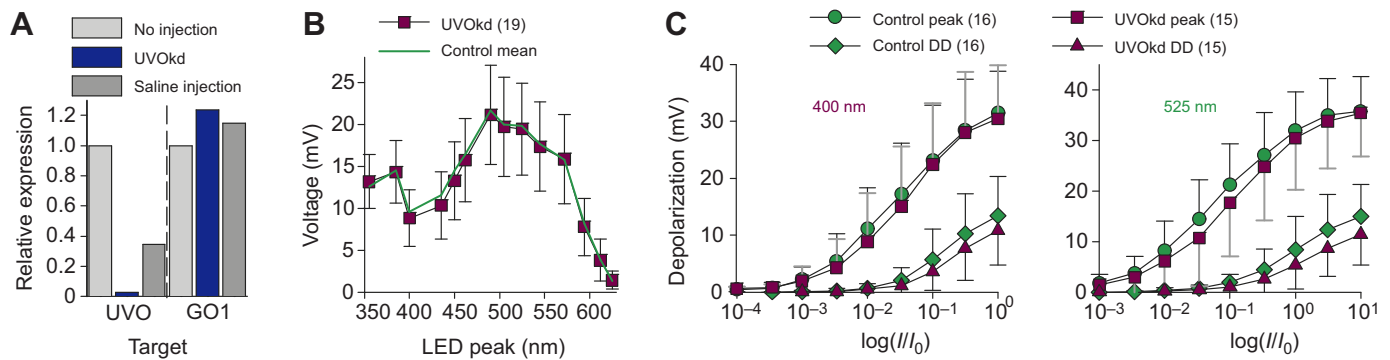


Fig. 5. UVO knockdown and its effects on green-sensitive photoreceptors. (A) UVOkd reduced UVO but not GO1 mRNA concentrations. Data were obtained by quantitative PCR using the means of actin and GAPDH mRNA abundances as reference compared with sham-injected and non-injected controls. Data were normalized with respect to control values; values are means of three technical replicates. (B) Average voltage responses of green-sensitive photoreceptors from UVOkd cockroaches to 20 ms isoquantal flashes of light from 14 LEDs. Data were obtained in intracellular experiments; the green line is the mean control action spectrum for green-sensitive photoreceptors from Fig. 1C. (C) Dependencies of peak and delayed depolarization (DD) on light level in control and UVOkd photoreceptors after stimulation with 20 ms violet (left) or green (right) stimuli. Values were determined as in Fig. 1F.

and delayed depolarization amplitudes on light level. Strong hyperpolarizations and delayed depolarizations were found in UV-sensitive photoreceptors after stimulation with 20 ms pulses at 525 nm in control (Fig. 1E) and UVOkd (Fig. 6E) but not in GO1/UVOkd (Fig. 6F) or GO1kd (Fig. 6G) cockroaches. When the hyperpolarization (Fig. 6H) and delayed depolarization (Fig. 6I) amplitudes from all experiments were compared, it was clear that knockdown of the green opsin removed these responses from most photoreceptors. These results suggest that the biphasic responses in UV-sensitive photoreceptors are mainly caused by activation of green-sensitive photoreceptors.

Angular sensitivity measurements

The source of delayed depolarization could be clarified by measuring angular sensitivity: if the effects were confined to the same ommatidium as the recorded photoreceptor, then the angular sensitivities obtained from the normal transient and the delayed depolarizations would be similar. If delayed depolarizations were caused by the activation of the neighboring ommatidia by the relatively wide light source used in these experiments (angular size of ca. 2.5 deg), then the angular sensitivity of the delayed depolarization would be substantially wider than the angular sensitivity obtained from the normal transient depolarizations.

Fig. 7A demonstrates responses of a normal green-sensitive photoreceptor to 100 ms pulses of violet light (400 nm) delivered at eight polar angles. Delayed depolarization was very strong in this photoreceptor and lasted for several seconds. Dependencies of the relative sensitivity on the polar angle fitted with first-order Gaussian functions are shown in Fig. 7B. The angular sensitivities are nearly identical. The acceptance angles ($\Delta\theta$) were determined as half-widths of the fitted Gaussians. The $\Delta\theta$ values for the normal transient and delayed depolarization responses in the dark-adapted green-sensitive photoreceptors after stimulation with 400 nm flashes were 7.6 ± 2.0 and 8.5 ± 3.4 deg ($n=6$), respectively. The corresponding values for stimulation with green light were 7.8 ± 1.9 and 5.9 ± 1.8 deg ($n=5$), respectively (Fig. 7C). The $\Delta\theta$ values for delayed depolarization after stimulation with green light were significantly narrower than for peak responses (paired t -test, $P=0.004$; Fig. 7C). The $\Delta\theta$ values for transient depolarization are consistent with previous reports of angular sensitivity in *P. americana* (Butler and Horridge, 1973; Heimonen et al., 2006).

However, the angle at which the maximal delayed depolarization was observed in green-sensitive photoreceptors stimulated with violet

did not match the angle of the maximal transient depolarization (Fig. 7A,B). On average, the mismatch between the peaks of fitted Gaussian functions was 1.33 ± 0.70 deg (absolute values used, $n=6$). In contrast, no significant mismatch was observed for delayed depolarization elicited in green-sensitive photoreceptors by green light: the mismatch was only 0.32 ± 0.26 deg (unpaired t -test, $P=0.014$, $n=5$; Fig. 7D). These results suggest that the cellular sources of the transient and delayed depolarizations by violet light are distinct.

DISCUSSION

We discovered anomalous responses in *P. americana* photoreceptors that indicate electrical interactions which, in turn, could modify the functioning of neighboring photoreceptors in relatively bright light. Electrical coupling between photoreceptors has been reported in several invertebrate species, including flies, locusts, honeybees, butterflies and crickets (Chen et al., 2013; Frolov et al., 2014; Matic, 1983; Schnaitmann et al., 2018; Shaw, 1969, 1975; Weckstrom and Laughlin, 2010). The consequences of such interactions for photoreceptor functioning are of interest because these responses are often quite large. Here, by selectively suppressing expression of two major opsin genes, we achieved some mechanistic insights into the nature of these anomalous responses and determined their local, intra-ommatidial origin.

A putative mechanism of interactions between photoreceptors

We found two electrophysiological phenomena: fast hyperpolarization and delayed depolarization. In the normal UV-sensitive photoreceptors stimulated with green light, and in green-sensitive photoreceptors from GO1kd cockroaches stimulated with UV/violet light, transient hyperpolarization was almost always followed by slow delayed depolarization, comprising a biphasic response. The hyperpolarization resembles the color-opponent responses reported in butterfly photoreceptors (Chen et al., 2013; Matic, 1983), and may be explained by similar mechanism (see below). To the best of our knowledge, the delayed depolarization is reported here for the first time. Owing to its slow kinetics, it cannot be explained by direct electrical interactions between photoreceptors. Instead, our results indicate that it is mediated by electric fields originating from depolarization of other photoreceptors in the same ommatidium. Most importantly, the hyperpolarizing component was eliminated and the delayed depolarization significantly reduced in

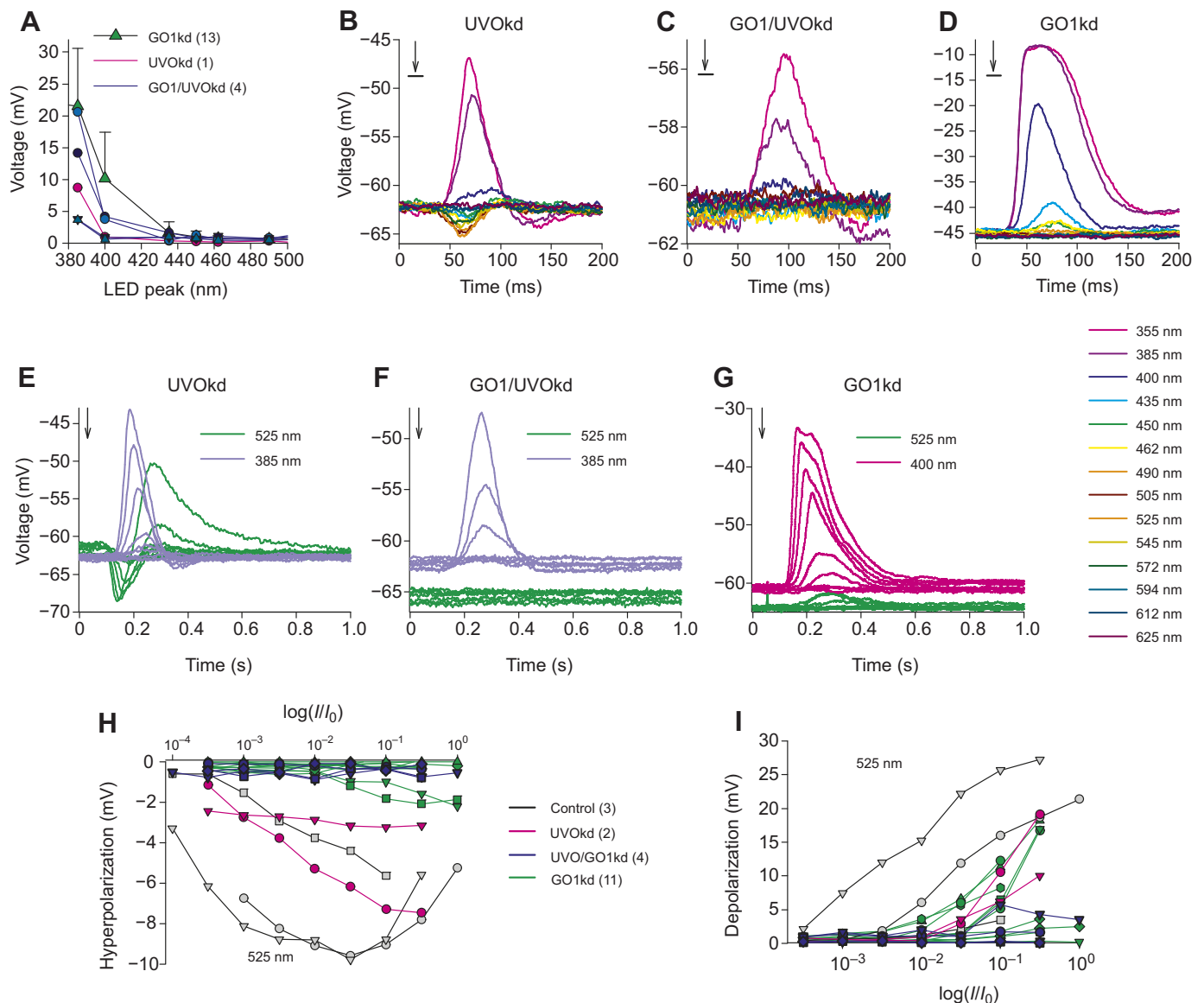


Fig. 6. Effects of opsin knockdowns in UV-sensitive photoreceptors. Data were obtained from intracellular experiments. (A) Mean dependencies of voltage transient amplitudes on peak LED wavelength for 13 UV-sensitive GO1kd photoreceptors, one UVOKd photoreceptor and individual responses of four UV-sensitive GO1/UVOKd photoreceptors. (B–D) Examples of responses to isoquantal stimulation with different LEDs. Color key is below D. (E–G) Responses of UV-sensitive UVOKd (E), GO1/UVOKd (F) and GO1kd (G) photoreceptors to 20 ms flashes of 525 or 400 nm light over a 10^4 range of light intensities. (H, I) Dependencies on light intensity of amplitudes of hyperpolarization (H) or delayed depolarization (I) are shown for 20 UV-sensitive photoreceptors stimulated with green light as in E–G. At the relative light level 10^{-1} in H, mean hyperpolarization amplitude was -6.8 ± 2.4 mV in the combined control and UVOKd group ($n=5$) versus -0.4 ± 0.4 mV in the combined GO1 and GO1/UVOKd group ($n=15$; $P=0.004$, unpaired t -test). The amplitude of delayed depolarization (I) decreased to a lesser extent, from 12.4 ± 8.8 mV in the combined control and UVOKd group ($n=5$) to 4.4 ± 4.1 mV in the combined GO1 and GO1/UVOKd group ($n=15$; $P=0.02$, unpaired t -test).

UV-sensitive photoreceptors after GO1 knockdown. The study of biphasic responses in broadband photoreceptors provided consistent but less conclusive results owing to inherent sensitivity of these photoreceptors to UV/violet light.

We suggest that the biphasic responses may be caused by the effects of changing ionic conditions on the electromotive force that drives the ions through the K^+ channel with the largest influence on the resting membrane potential, the EAG K^+ channel. We have shown previously that the *P. americana* photoreceptor resting membrane potential depends on these channels (Immonen et al., 2017). The EAG channels have a substantial permeability to Na^+ ions. The $Na^+:K^+$ selectivity ratio for *P. americana* EAG is not

known, but using the value of 0.11 from *Drosophila melanogaster* EAG, under the ionic conditions in our patch-clamp recordings, the equilibrium potential for EAG channels would be -51.5 mV as calculated using the Goldman–Hodgkin–Katz equation, 5.5 mV above the actual resting membrane potential (-57 ± 6 mV) in our patch-clamp experiments.

The microvillar arrays in the fused rhabdom ommatidia are tightly interlocked and the intra-ommatidial extracellular space is restricted (Frolov et al., 2017). It is possible that under such conditions, opening of ion channels can disturb the intra-ommatidial extracellular ionic concentrations. If a robust inward current through light-activated channels in the rhabdom lowered the

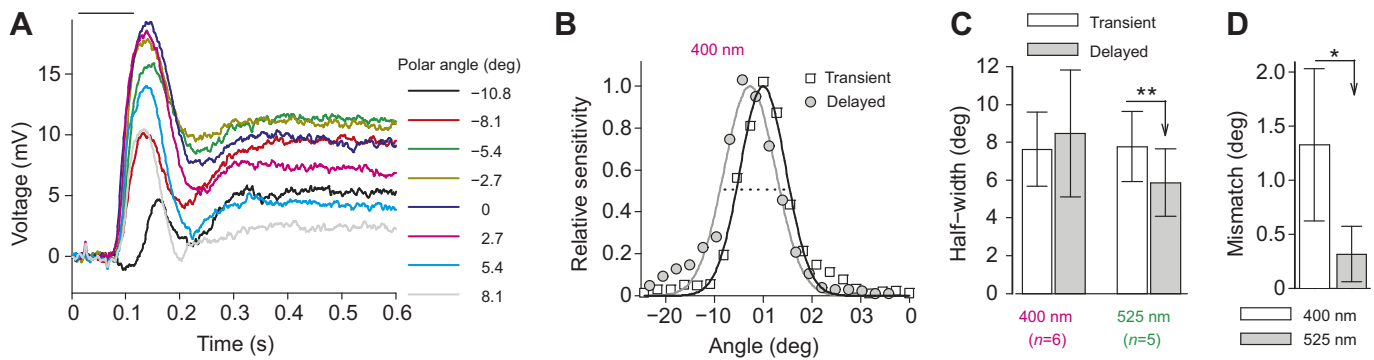


Fig. 7. Angular sensitivity of the primary and delayed depolarization responses. Data were obtained from intracellular recordings from green-sensitive photoreceptors. (A) Responses to a 100 ms violet (400 nm) pulse (horizontal line) at eight polar angles during measurement of angular sensitivity; traces are provided for the largest responses only; key denotes adjusted polar angles. Blue trace shows a response with the highest transient depolarization, and green the response with the maximal delayed depolarization. Resting potentials were subtracted. (B) Angular sensitivity data points for the same photoreceptor as in A fitted with first-order Gaussian functions. (C) Mean acceptance angles for the transient and delayed depolarization determined as half-widths of the Gaussian fits for responses elicited by violet or green light as indicated. (D) Mean discrepancies between angular sensitivity peaks for the transient and delayed depolarization responses of green-sensitive photoreceptors stimulated with either violet or green light. Significant differences indicated at * $P < 0.05$ and ** $P < 0.01$, paired t -test.

extracellular Na^+ concentration by 10 mmol l^{-1} (from 120 to 110 mmol l^{-1}), the equilibrium potential created by EAG channels would shift by -1.5 mV . If repolarizing K^+ channels opened in the neighboring light-activated photoreceptors, the external K^+ concentration would increase from 5 to 15 mmol l^{-1} , and then the equilibrium potential for EAG would shift by $+11 \text{ mV}$. Because some EAG channels are open at rest, these changes in concentrations would lead to ionic currents, with their kinetics closely following the time courses of the causative events. However, as hyperpolarization would tend to deactivate EAG channels, while depolarization would activate them, this interplay of negative and positive feedbacks would result in relatively small hyperpolarizing and high depolarizing components of the ephaptic response.

In addition to explaining the biphasic responses, this mechanism could account for the phenomenon of prolonged delayed depolarizations after short flashes of relatively bright green light often observed in intracellular recordings from green-sensitive photoreceptors (Fig. 1F, green and cyan traces). If extracellular K^+ concentration were to rise because of strong concerted opening of voltage-gated K^+ channels in abutting photoreceptors, then this transiently high extracellular K^+ concentration would set a new resting potential, which would gradually return to normal as the locally elevated K^+ concentration dissipates.

We did not find delayed depolarization in patch-clamp experiments after stimulating green-sensitive photoreceptors with bright UV light (Fig. 2). As photoreceptors in dissociated ommatidia lack axons, these results indicate only that the delayed depolarization is unlikely to be caused by any electrochemical process within the photoreceptor soma, e.g. caused by the Na^+/K^+ -ATPase or $\text{Na}^+/\text{Ca}^{2+}$ exchanger. The absence of delayed depolarization in patch-clamp experiments is not inconsistent with the intraommatidial ephaptic hypothesis proposed above. Because the retina dissociation involves intensive trituration after exposure to digestive enzymes, the normal ommatidial morphology is lost and some ommatidia fall apart completely. This decreases the electrical resistance in the intra-ommatidial space and alters the ionic concentrations.

The amplitudes of delayed depolarizations are large, up to tens of millivolts, suggesting that they are not caused by a general field potential in the excited retina as reported for the butterfly *Papilio* (Matić, 1983). Such effects usually have significantly smaller amplitudes (French et al., 2015). Therefore, the delayed

depolarizations in cockroach photoreceptors are more likely caused by interactions within the ommatidium or between neighboring ommatidia. Our hypothesis is supported by the finding that the mean acceptance angles for the primary and delayed depolarizations were similar in green-sensitive photoreceptors stimulated with violet light. Importantly, the peaks of the angular sensitivity functions for the normal transient and delayed depolarizations mismatched when photoreceptors were stimulated with violet but not with green light (Fig. 7). These observations suggest that the source of anomalous delayed depolarization is within the same ommatidium but unlikely to be the recorded photoreceptor.

If we assume that activation of adjacent green-sensitive photoreceptors results in delayed depolarization, then why are their amplitudes and time course different when stimulated with UV/violet versus green light? A number of factors may be involved: different channelomes in UV and green-sensitive photoreceptors (e.g. Frolov et al., 2014), or morphological differences. The latter possibility is interesting, because we found only a few UV-sensitive photoreceptors among hundreds recorded in our patch-clamp studies, while in intracellular recordings, UV-sensitive photoreceptors are encountered more frequently. In patch-clamp experiments, the electrode is advanced from the side and a certain amount of accessible membrane is necessary for seal formation, so such a discrepancy could be caused by UV-sensitive photoreceptors being less accessible for patching. For example, they may be much smaller or partly surrounded by the green-sensitive photoreceptors. In the latter situation, efflux of K^+ into the extracellular space during depolarization of UV-sensitive photoreceptors could produce larger and longer-lasting disturbances of interstitial ionic milieu than depolarization of green-sensitive photoreceptors.

Other possible mechanisms

Ephaptic coupling is a form of electrical interaction involving a contact between cells via an electrical field, which in living systems could arise from spatially and temporally disturbed ionic concentrations in the extracellular space. However, apart from local field interactions, electrical coupling between neurons may involve several other mechanisms.

The hypothesis presented above differs from the model developed by Shaw (1975) to explain lateral inhibition between photoreceptors in the locust, and later applied to butterfly (Chen

et al., 2013; Matić, 1983) and blowfly photoreceptors (Weckstrom and Laughlin, 2010). Shaw (1975) suggested that the basal membrane forming the proximal boundary of the retina constitutes a high resistance barrier in the extracellular space, so that ionic currents flowing along the photoreceptor and axon, and leaving through the synapse, can close the circuit only via the axons and somata of neighboring photoreceptors. This leads to transient hyperpolarization in the non-illuminated photoreceptor (Shaw, 1975). Although this mechanism is consistent with the hyperpolarization observed here, the delayed depolarization cannot be explained by this model. Although biphasic responses were observed in butterflies, their durations were no longer than the normal depolarizing transients (Matić, 1983).

Importantly, Matić (1983) showed that most hyperpolarizations (and possibly also depolarizations) measured in intracellular recording experiments could not be seen in differential recordings with the reference electrode in close proximity to the recording electrode in the extracellular space. Thus, whether the signals recorded here are the same or different to the passive signals that are conveyed through the axon or the synaptic output of the photoreceptors remains unknown.

Another putative mechanism could involve direct synaptic interactions between photoreceptors (Schnaitmann et al., 2018). However, if UV-sensitive photoreceptors form long visual fibers, which terminate in the second optic neuropil, the medulla, as occurs in the fruit fly (Ribi, 1977), then synaptic interactions between green- and UV-sensitive photoreceptors are unlikely. Another possibility could be direct interactions between photoreceptors of different spectral classes via gap junctions. This could explain the delayed depolarization if the connection between two cells had very high impedance and were therefore strongly low-pass filtering, but it could not explain the preceding hyperpolarization. Moreover, the absence of delayed depolarization in patch-clamp experiments indicates that no direct connections exist at the level of the cell body. This is in contrast to previous findings in *G. bimaculatus*, where two very distinct types of quantum bumps were observed in patch-clamp experiments – normal high-amplitude ones and small bumps with very slow kinetics – suggesting direct coupling between green-sensitive photoreceptors (Frolov et al., 2014).

Competing interests

The authors declare no competing or financial interests.

Author contributions

Conceptualization: R.F.; Methodology: R.F.; Formal analysis: P.S., H.L., R.F.; Investigation: P.S., E.I., H.L., K.H., R.F.; Writing - original draft: R.F.; Writing - review & editing: P.S., A.F., P.T., R.F.; Supervision: P.T., R.F.; Project administration: A.F., P.T., R.F.; Funding acquisition: A.F., P.T.

Funding

This research was funded by the Natural Sciences and Engineering Research Council of Canada (RGPIN/05565 to P.T. and RGPIN/03712 to A.S.F.).

References

- Butler, R. and Horridge, G. A. (1973). The electrophysiology of the retina of *Periplaneta americana* L. *J. Comp. Phys.* **83**, 263–278.
- Chen, P.-J., Arikawa, K. and Yang, E.-C. (2013). Diversity of the photoreceptors and spectral opponency in the compound eye of the golden birdwing, *Troides aeacus formosanus*. *PLoS ONE* **8**, e62240.
- French, A. S., Meisner, S., Liu, H., Weckstrom, M. and Torkkeli, P. H. (2015). Transcriptome analysis and RNA interference of cockroach phototransduction indicate three opsins and suggest a major role for TRPL channels. *Front. Physiol.* **6**, 207.
- Frolov, R.-V., Immonen, E. V. and Weckstrom, M. (2014). Performance of blue- and green-sensitive photoreceptors of the cricket *Gryllus bimaculatus*. *J. Comp. Physiol. A* **200**, 209–219.
- Frolov, R.-V., Matsushita, A. and Arikawa, K. (2017). Not flying blind: a comparative study of photoreceptor function in flying and non-flying cockroaches. *J. Exp. Biol.* **220**, 2335–2344.
- Heimonen, K., Salmela, I., Kontiokari, P. and Weckstrom, M. (2006). Large functional variability in cockroach photoreceptors: optimization to low light levels. *J. Neurosci.* **26**, 13454–13462.
- Henze, M. J., Dannenhauer, K., Kohler, M., Labhart, T. and Gesemann, M. (2012). Opsin evolution and expression in arthropod compound eyes and ocelli: insights from the cricket *Gryllus bimaculatus*. *BMC Evol. Biol.* **12**, 1–16.
- Immonen, E. V., French, A. S., Torkkeli, P. H., Liu, H., Vahasoyrinki, M. and Frolov, R. V. (2017). EAG channels expressed in microvillar photoreceptors are unsuited to diurnal vision. *J. Physiol.* **595**, 5465–5479.
- Johnson, E. C. and Pak, W. L. (1986). Electrophysiological study of *Drosophila* rhodopsin mutants. *J. Gen. Physiol.* **88**, 651–673.
- Kamermans, M. and Fahrenfort, I. (2004). Ephaptic interactions within a chemical synapse: hemichannel-mediated ephaptic inhibition in the retina. *Curr. Opin. Neurobiol.* **14**, 531–541.
- Matić, T. (1983). Electrical inhibition in the retina of the butterfly *Papilio*. *J. Comp. Phys.* **152**, 169–182.
- Mote, M. I. and Goldsmith, T. H. (1970). Spectral sensitivities of color receptors in the compound eye of the cockroach *Periplaneta*. *J. Exp. Zool.* **173**, 137–145.
- Mote, M. I. and Goldsmith, T. H. (1971). Compound eyes: localization of two color receptors in the same ommatidium. *Science* **171**, 1254–1255.
- Ribi, W. A. (1977). Fine structure of the first optic ganglion (lamina) of the cockroach, *Periplaneta americana*. *Tissue Cell* **9**, 57–72.
- Saari, P., French, A. S., Torkkeli, P. H., Liu, H., Immonen, E.-V. and Frolov, R. V. (2017). Distinct roles of light-activated channels TRP and TRPL in photoreceptors of *Periplaneta americana*. *J. Gen. Physiol.* **149**, 455–464.
- Schnaitmann, C., Haikala, V., Abraham, E., Oberhauser, V., Thestrup, T., Griesbeck, O. and Reiff, D. F. (2018). Color processing in the early visual system of *Drosophila*. *Cell* **172**, 318–330.e18.
- Shaw, S. R. (1969). Interreceptor coupling in ommatidia of drone honeybee and locust compound eyes. *Vision Res.* **9**, 999–1029.
- Shaw, S. R. (1975). Retinal resistance barriers and electrical lateral inhibition. *Nature* **255**, 480–482.
- Stavenga, D. G., Smits, R. P. and Hoenders, B. J. (1993). Simple exponential functions describing the absorbance bands of visual pigment spectra. *Vision Res.* **33**, 1011–1017.
- Vroman, R., Klaassen, L. J. and Kamermans, M. (2013). Ephaptic communication in the vertebrate retina. *Front. Hum. Neurosci.* **7**, 612.
- Weckstrom, M. and Laughlin, S. (2010). Extracellular potentials modify the transfer of information at photoreceptor output synapses in the blowfly compound eye. *J. Neurosci.* **30**, 9557–9566.